Original Article

Asian Pacific Journal of Tropical Biomedicine

journal homepage: www.apjtb.org

doi: 10.4103/2221-1691.350180

Impact Factor: 1.51

Anticancer activity of Δ^9-tetrahydrocannabinol and cannabinol *in vitro* and in human lung cancer xenograft

Surang Leelawat[1]✉, Kawin Leelawat[2], Thaniya Wannakup[3], Worawan Saingam[3], Nanthaphong Khamthong[4], Fameera Madaka[3], Athip Maha[3], Patamaporn Pathompak[3], Lukman Sueree[3], Thanapat Songsak[5]

[1]*Medicinal Cannabis Research Institute, College of Pharmacy, Rangsit University, Pathum Thani 12000, Thailand*

[2]*Department of Surgery, Bumrungrad International Hospital, Bangkok 10110, Thailand*

[3]*Drug and Herbal Product Research and Development Center, College of Pharmacy, Rangsit University, Pathum Thani 12000, Thailand*

[4]*College of Oriental Medicine, Rangsit University, Pathum Thani 12000, Thailand*

[5]*Department of Pharmacognosy, College of Pharmacy, Rangsit University, Pathum Thani 12000, Thailand*

ABSTRACT

Objective: To investigate the effects of Δ^9-tetrahydrocannabinol, the principal psychoactive compound of *Cannabis sativa*, and cannabinol, a Δ^9-tetrahydrocannabinol degradative product, on human non-small cell lung cancer cells.

Methods: Δ^9-Tetrahydrocannabinol and cannabinol were tested for anticancer activity in human non-small cell lung cancer (A549) cells. The effects on cell proliferation, apoptosis, and phosphorylation profiles were examined. The effects of Δ^9-tetrahydrocannabinol and cannabinol on tumor growth were also investigated using a xenograft nude mouse model. Apoptosis and targeted phosphorylation were verified by immunohistochemistry.

Results: Δ^9-Tetrahydrocannabinol and cannabinol significantly inhibited cell proliferation and increased the number of apoptotic cells in a concentration-dependent manner. The Δ^9-tetrahydrocannabinol- and cannabinol-treated cells had lower levels of phosphorylated protein kinase B [AKT (S473)], glycogen synthase kinase 3 alpha/beta, and endothelial nitric oxide synthase compared to the controls. The study of xenograft mice revealed that tumors treated with 15 mg/kg Δ^9-tetrahydrocannabinol or 40 mg/kg cannabinol were significantly smaller than those of the control mice. The tumor progression rates in mice treated with 15 mg/kg Δ^9-tetrahydrocannabinol or 40 mg/kg cannabinol were significantly slower than in the control group.

Conclusions: These findings indicate that Δ^9-tetrahydrocannabinol and cannabinol inhibit lung cancer cell growth by inhibiting AKT and its signaling pathways, which include glycogen synthase kinase 3 alpha/beta and endothelial nitric oxide synthase.

KEYWORDS: Cannabis; Δ^9-Tetrahydrocannabinol; Cannabinol; Non-small cell lung cancer; AKT; *Cannabis sativa;* Glycogen synthase kinase 3 alpha/beta; Endothelial nitric oxide synthase

1. Introduction

Lung cancer is common cancer worldwide and a major cause of mortality in men and women[1]. The most common type of lung cancer is non-small cell lung cancer (NSCLC). Surgery is

Significance

Δ^9-Tetrahydrocannabinol, the major psychoactive component of *Cannabis sativa*, has been demonstrated to inhibit cancer cell proliferation and invasion, as well as to induce apoptosis. Cannabinol, an oxidative byproduct of Δ^9-tetrahydrocannabinol, has a weak psychotropic potency. In the current study, Δ^9-tetrahydrocannabinol and cannabinol inhibited non-small cell lung cancer cell proliferation and induced apoptosis by inhibiting AKT, glycogen synthase kinase 3 alpha/beta, and endothelial nitric oxide synthase, and inhibiting tumor growth in xenograft mice by inducing tumor cell apoptosis.

✉To whom correspondence may be addressed. E-mail: surang.l@rsu.ac.th

How to cite this article: Leelawat S, Leelawat K, Wannakup T, Saingam W, Khamthong N, Madaka F, et al. Anticancer activity of Δ^9-tetrahydrocannabinol and cannabinol *in vitro* and in human lung cancer xenograft. Asian Pac J Trop Biomed 2022; 12(8): 323-332.

Article history: Received 1 March 2022; Revision 1 April 2022; Accepted 31 May 2022; Available online 23 July 2022

the treatment of choice for the early stages of NSCLC. However, 70% of patients present with advanced-stage disease at the time of diagnosis[2].

Traditional chemotherapeutic drugs appear to be ineffective for the treatment of advanced-stage NSCLC. Targeting epidermal growth factor receptor (EGFR) and other signal transduction pathways have been identified as a potential therapeutic strategy for advanced-stage NSCLC[2]. Previous research has found that the phosphatidylinositol 3 kinase (PI3K)-protein kinase B (AKT) pathway is activated in at least 14.9% of EGFR tyrosine kinase inhibitors (EGFR-TKI)-resistant patients[3]. The presence of PI3K-related mutations in conjunction with EGFR-activating mutations indicates a poor prognosis and predicts a shorter progression-free survival period with EGFR-TKI treatment[3]. Thus, novel therapeutics for NSCLC that target the PI3K-AKT pathway are required.

To date, the anticancer molecular mechanisms of cannabinoids have been demonstrated[4,5]. Δ^9-Tetrahydrocannabinol (THC), the major psychoactive constituent of *Cannabis sativa* (marijuana), induces cancer cell apoptosis *via* the CB1 and CB2 receptors. The activation of CB1 and CB2 receptors inhibits AKT, which leads to the inhibition of mammalian target of rapamycin complex 1 and, eventually, cell apoptosis[6].

Cannabinoids have previously been shown to induce autophagy in several cancer cell lines, including glioma, melanoma, and hepatic and pancreatic cancer[6]. In addition, our previous report demonstrated that THC inhibits cell proliferation, migration, and invasion, and induces apoptosis in cholangiocarcinoma cells by decreasing actin polymerization and inhibiting the MEK1/2 and AKT pathways[7]. Nonetheless, epidemiological studies provide sufficient evidence to warrant a public health warning that cannabis use, particularly of high potency types, can increase the risk of psychotic disorders[8]. Cannabinol (CBN), a byproduct of the non-enzymatic oxidation of THC, has demonstrated anticonvulsant and anti-inflammatory properties. In comparison to THC, CBN has fewer psychoactive effects and a lower binding affinity for the CB1 receptor[9]. While the preclinical evidence for potential anticancer of THC is encouraging, the elucidation of underlying molecular mechanisms of CBN in preclinical study still has to be fully identified. Thus, the purpose of this study is to evaluate the effects of THC and CBN in human lung cancer xenograft mouse models and to examine the mechanisms of THC and CBN actions in a human NSCLC cell line.

2. Materials and methods

2.1. Materials

Polyclonal antibodies against AKT (phosphorylated at Ser473) (cat. no. 9271), glycogen synthase kinase 3 alpha/beta (GSK-3α/β) (phosphorylated at Ser21/9) (cat. no. 9331), endothelial nitric oxide synthase (eNOS) (phosphorylated at Ser1177) (cat. no. 9571), poly (ADP-ribose) polymerase [PARP (46D11)] (cat. no. 9532), cleaved PARP (Asp214) (cat. no. 5625), caspase-3, cleaved caspase-3 (Asp175) (cat. no. 9661), and β-actin (cat. no. 4967), and anti-rabbit immunoglobulin G (IgG) horseradish peroxidase (HRP)-linked antibody (cat. no. 7074), LY294002, *L*-NAME, radioimmunoprecipitation assay buffer, and protease inhibitor cocktail were purchased from Cell Signaling Technology (Beverly, MA, USA). RPMI 1640 medium and fetal bovine serum (FBS) were purchased from Gibco (Grand Island, NY, USA). Culture plates and flasks were purchased from Falcon (Corning, NY, USA). Matrigel basement membrane matrix was purchased from Corning (Corning, NY, USA). The Bradford protein assay was purchased from Bio-Rad (Hercules, CA, USA).

2.2. Cell cultures

The human NSCLC cell line A549 (ATCC® CCL-185™; Manassas, VA, USA) was grown in RPMI 1640 medium supplemented with 10% FBS at 37℃ in a 5% CO_2 humidified atmosphere.

2.3. Analysis of THC and CBN

THC and CBN were extracted from dried cannabis samples in-house at the College of Pharmacy, Rangsit University. The identities of the compounds were verified by comparing their ^{1}H- and ^{13}C-NMR data to that in the literature and matching their mass spectral data to that in the NIST database. High-performance liquid chromatography (HPLC) was used to determine the purity quantitatively [Prominence UFLC, Shimazu, Japan; mobile phase: (ammonium formate: acetonitrile), gradient elution, flow rate 1.0 mL/min, column: XBridge C18, detection at 228 nm].

2.4. Cell proliferation assay

A549 cells were seeded in 96-well flat-bottom plates at a concentration of 1×10^4 cells/well in 100 μL of culture medium containing 10% FBS for 24 h at 37℃ in an atmosphere of 5% CO_2. After the incubation period, cells were treated with various amounts of THC or CBN (at final concentrations of 10-100 μM), LY294002 (a selective inhibitor of PI3K, 10-20 μM), *L*-NAME (a NOS inhibitor, 1-10 μM), or vehicle. After incubation for 24 h or 48 h, 50 μL of 3-(4,5-dimethyl thiazol-2-yl)-2-5-diphenyltetrazolium bromide (MTT; Sigma-Aldrich, Germany) at 0.5 mg/mL in phosphate buffered saline (PBS) was applied to each well. The reaction was measured at 590 nm using a Benchmark Plus microplate reader (Bio-Rad).

2.5. Detection of cell apoptosis

Apoptotic cells were evaluated by flow cytometric analysis using an annexin V:FITC assay (Bio-Rad). A549 cells were seeded at 1×10^6 cells per sample. The cells were then treated with vehicle, THC, or CBN at 10 μM and 20 μM for 18 h. After the incubation period, the cells were collected. The annexin V:FITC assay was performed following the protocol specified by the manufacturer. Briefly, the treated cells were harvested, washed in PBS, resuspended at 5×10^5 cells/mL in 200 μL of binding buffer containing 5 μL annexin V:FITC, and incubated for 10 min in the dark at room temperature. Next, the cells were washed in binding buffer, resuspended in 200 μL of binding buffer containing 10 μL propidium iodide solution, and analyzed by flow cytometry (BD FACSVerse Flow Cytometer, BD Biosciences, Franklin Lakes, NJ, USA).

2.6. Detection of phosphokinase signaling pathways

To analyze the phosphorylation profiles, A549 cells at 1×10^7 were starved in a serum-free medium overnight. These cells were then treated with vehicle or 20 μM of THC or CBN for 18 h. After the incubation period, the cells were analyzed using a Proteome Profiler Array Human Phospho-Kinase Array Kit (R&D Systems, Inc., Minneapolis, MN, USA) following the manufacturer's instructions. Briefly, the cell lysate was diluted and incubated overnight with the Human Phospho-Kinase Array membrane. The array membrane was washed to remove unbound proteins and then incubated with a cocktail of biotinylated detection antibodies. After washing, streptavidin-HRP and chemiluminescent detection reagents were applied. A chemiluminescent signal produced at each capture spot corresponding to the amount of phosphorylated protein bound was captured using UVP ChemStudio (Analytik, Jena, Germany) and analyzed using ImageJ digital imaging processing software (ImageJ 1.48v, National Institutes of Health, Bethesda, MD, USA). The intensity of each signal was calculated relative to the reference signal of the array kit. The relative change in phosphorylated kinase proteins was examined between control and treatment samples.

2.7. Western blotting analyses

A549 cells were seeded at 5×10^5 cells/well in a six-well culture plate. The cells were then treated with vehicle, THC, or CBN at 10 μM or 20 μM for 18 h. Treated cells were trypsinized, washed with PBS, and lysed in ice-cold radioimmunoprecipitation assay buffer containing a 1% protease inhibitor cocktail, followed by sonication for 10 s. The protein concentration of the cell lysate supernatant was determined using a Bradford assay. Western blot analyses were performed as previously described[7]. The membranes were incubated overnight at 4 ℃ with primary antibodies against phosphorylated AKT, GSK-3α/β, eNOS, PARP (46D11), cleaved PARP, and β-actin at the dilution of 1:1 000. Following the manufacturer's instructions, colorimetric detection of the target proteins on the membrane was performed using an Opti-4CN Detection Kit (Bio-Rad).

2.8. Xenograft mice

Four-week-old female athymic nude mice (BALB/cAJcl-Nu/Nu) were obtained from Nomura Siam International Co., Ltd. (Bangkok, Thailand) and were housed under specific pathogen-free conditions with a 12-hour light/dark cycle, (50±20)% humidity, and a temperature of (21±1) ℃. Following acclimatization, A549 cells at 3×10^6 cells in 100 μL serum-free RPMI 1640 medium and 100 μL Matrigel basement membrane matrix were injected subcutaneously into the right flank to establish the xenograft tumor model. The tumors were allowed to develop until they reached an average volume of 150 mm^3. Mice were then randomized into treatment groups of five animals per group, including an untreated control group (1% Tween 80) and three groups treated with cannabinoids (15 mg/kg THC, 20 mg/kg CBN, and 40 mg/kg CBN based on our pilot study). The mice were given daily subcutaneous injections of either 1% Tween 80 or cannabinoids for 20 d. The tumors were assessed twice weekly by measuring the length and width with standard calipers and calculating the tumor volume using the formula $(L \times W \times W)/2$, where L is the long diameter of the tumor and W is the short diameter of the tumor. The body weight of the mice was also measured twice a week. Mice were euthanized by carbon dioxide and cervical dislocation at the end of the treatment. Tumors were obtained and preserved in 10% buffered formalin for histopathological and immunohistochemical analyses.

2.9. Immunohistochemistry

The paraffin-embedded specimen sections were deparaffinized in xylene and rehydrated in ethanol, followed by water. The endogenous peroxidase in the tissue was then blocked using a hydrogen peroxide blocking reagent (Abcam, Cambridge, UK). After washing, antigen retrieval was performed by heating the sections in 10 mM citrate buffer solution (pH 6.0). After storage at room temperature, the sections were washed, and a protein block solution (Abcam, Cambridge, UK) was applied to reduce nonspecific background staining. The sections were then washed and incubated with primary antibodies in a humidified chamber. After overnight incubation, the antigen-antibody complex was detected using a Mouse and Rabbit Specific HRP/DAB (ABC) Detection IHC Kit (Abcam, Cambridge, UK) according to the manufacturer's instructions. The sections were counterstained with a hematoxylin and eosin solution (Abcam, Cambridge, UK). For negative control, the primary antibody was substituted with SignalStain antibody diluent (Cell Signaling Technology). The stained sections were

examined under a Motic BA210 microscope (Schertz, TX, USA).

2.10. Statistical analysis

The studies were all done in triplicate and the data are presented as means with standard deviations. One-way analysis of variance (ANOVA) was used to compare data between three or more groups, followed by Dunnett's *post hoc* tests. The rate of xenograft tumor progression (assessed by the number of mice with a tumor volume < 300 mm^3) was evaluated using survival curves and compared using the log-rank test. Statistical significance was defined as a *P*-value less than 0.05.

2.11. Ethical statement

All animal studies followed the protocol approved by the Institutional Care and Use Committee of Rangsit University (approval number 103/2561) under Ethical Principles and Guidelines for the Use of Animals, National Research Council of Thailand.

3. Results

3.1. Characterization of THC and CBN

THC and CBN were isolated as yellow gum. The GC-MS spectrum of THC (Figure 1A) exhibited $[M]^+$, $[M\text{-}CH_3]^+$ and $[M\text{-}C_3H_7]^+$ ions at *m/z* values of 314, 299, and 271, respectively. The GC-MS spectrum of CBN (Figure 1B) exhibited $[M]^+$ and $[M\text{-}CH_3]^+$ ions at *m/z* values of 310 and 295, respectively. The identity of THC and CBN was confirmed by ^{1}H- and ^{13}C-NMR data. Figures 1C and 1D show the ^{1}H- and ^{13}C-NMR of THC, and Figures 1E and 1F show the ^{1}H- and ^{13}C-NMR of CBN. The ^{1}H- and ^{13}C-NMR data of THC and CBN were almost identical to those reported in a previous study[10]. According to HPLC analyses, the THC purity was 99.31% (Figure 1G) and the CBN purity was 99.76% (Figure 1H).

3.2. Effects of THC and CBN on cell proliferation

A cell proliferation assay was performed using human lung cancer cells (A549) with CBN and THC applied at 10-100 μM or vehicle. THC and CBN decreased cell proliferation in a concentration-dependent manner (Table 1). CBN showed anti-proliferative effects with IC_{50} values of 19.24 μM at 24 h and 14.96 μM at 48 h. THC showed similar anti-proliferative effects with IC_{50} values of 26.94 μM at 24 h and 21.90 μM at 48 h.

3.3. Effects of THC and CBN on cell apoptosis

Apoptotic cell death was determined by flow cytometric analysis using an annexin V:FITC assay. Treating A549 cells with 20 μM of CBN significantly increased the number of apoptotic cells (*P*=0.004 *vs*. control cells). Treating A549 cells with 10 μM and 20 μM THC also significantly increased the number of apoptotic cells [*P*=0.002 for 10 μM and *P*<0.001 for 20 μM, *vs*. control cells (Figures 2A and B)].

To confirm apoptotic cell death after treatment with cannabinoids, detection of the cleaved PARP protein in treated A549 cells was performed using Western blotting analysis. Cleaved PARP protein was found in A549 cells treated with 20 μM CBN and 10 μM THC (Figure 2C).

3.4. Effects of THC and CBN on cancer cell signaling

Analysis of the phosphorylation profiles of kinases is crucial for identifying the responses of cancer cells to environmental changes. The Human Phospho-Kinase Array was used to simultaneously detect the relative phosphorylation levels of 43 kinase phosphorylation sites and two related total proteins. The results showed that CBN- and THC-treated cells expressed less of some target proteins (Figure 3A).

Phosphorylated AKT (S473), GSK-3α/β, and eNOS were selected for Western blot analysis to verify the signals involved in cell proliferation and apoptosis. Western blot analysis showed that the phosphorylation of AKT (S473), GSK-3α/β, and eNOS was substantially decreased in CBN- and THC-treated cells at concentrations of 10 μM and 20 μM (Figure 3B). These results suggest that the AKT and eNOS pathways are inhibited in CBN- and THC-treated cells.

In addition, specific inhibitors of AKT (LY294002) or eNOS (*L*-NAME) were applied and a proliferation assay was used to investigate whether the AKT or eNOS pathways are associated with cell viability. The results indicated that LY294002 significantly decreased the viability of A549 cells at 10 μM and 20 μM at 24 h (*P*=0.030 for 10 μM and *P*=0.002 for 20 μM) and 48 h compared to the control cells (*P*=0.036 for 10 μM and *P*=0.001 for 20 μM).

Table 1. Effects of Δ^9-tetrahydrocannabinol and cannabinol on A549 lung cancer cell proliferation (%).

Time (h)	Cannabinol (μM)				Δ^9-Tetrahydrocannabinol (μM)			
	10	20	40	100	10	20	40	100
24	88.93±9.63	35.96±6.09	8.12±1.22	1.56±1.24	78.26±10.98	75.72±3.51	22.36±7.63	9.55±5.10
P-value	0.143	<0.001	<0.001	<0.001	0.022	0.002	<0.001	<0.001
48	76.15±15.98	29.4±6.86	5.23±1.56	1.25±0.75	65.9±18.95	58.78±13.02	4.33±2.04	2.37±1.16
P-value	0.041	<0.001	<0.001	<0.001	0.017	0.002	<0.001	<0.001

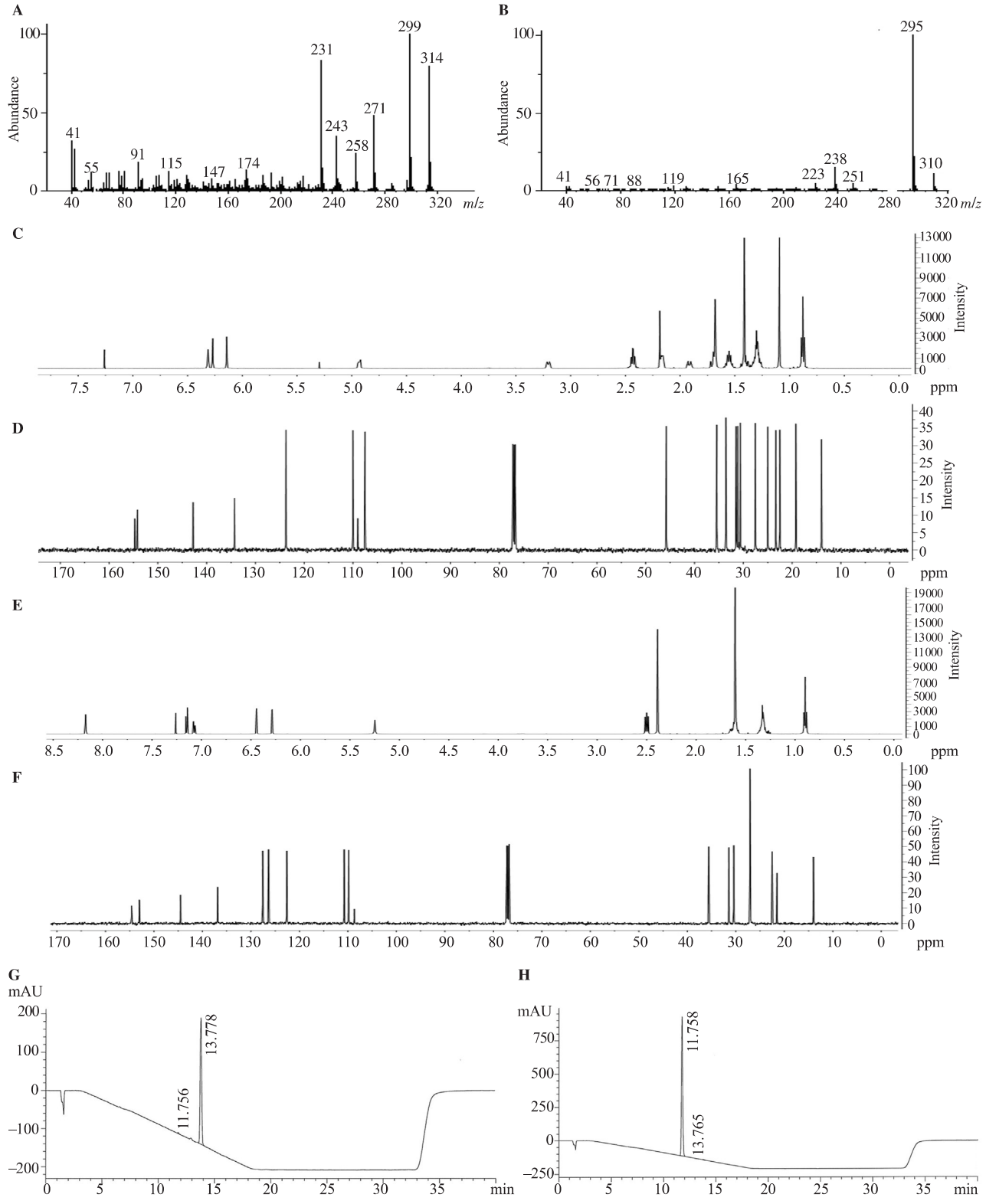

Figure 1. GC-MS spectra, ^{1}H- and ^{13}C-NMR spectra, and HPLC chromatograms for Δ^{9}-tetrahydrocannabinol (THC) and cannabinol (CBN). (A) GC-MS spectrum for THC. (B) GC-MS spectrum for CBN. (C) ^{1}H NMR spectrum (500 MHz, $CDCl_3$) for THC. (D) ^{13}C NMR spectrum (125 MHz, $CDCl_3$) for THC. (E) ^{1}H NMR spectrum (500 MHz, $CDCl_3$) for CBN. (F) ^{13}C NMR spectrum (125 MHz, $CDCl_3$) for CBN. (G) HPLC chromatogram for THC. (H) HPLC chromatogram for CBN.

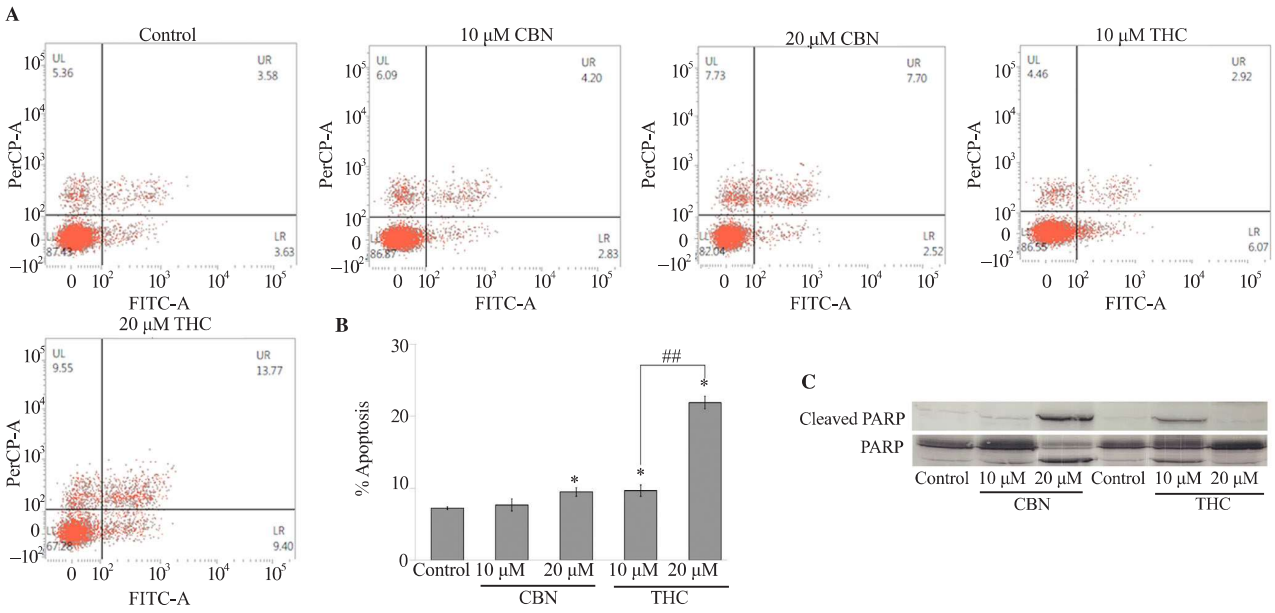

Figure 2. THC and CBN induce apoptosis in A549 lung cancer cells. (A) Flow cytometry data shows the percentage of live, apoptotic, and necrotic A549 cells after 18 h incubation with the vehicle, or THC or CBN at 10 μM or 20 μM. (B) Flow cytometry analysis demonstrated that THC at 10 μM and 20 μM, and CBN at 20 μM, significantly increase apoptotic cells compared to the control (ANOVA, $^{*}P<0.05$). In addition, 20 μM THC significantly increases the number of apoptotic A549 cells compared to 10 μM THC (ANOVA, $^{\#\#}P<0.001$). (C) Cleaved PARP in A549 lung cancer cells following 10 μM and 20 μM THC or CBN treatment for 18 h was determined by Western blot analysis. PARP was used as a loading control.

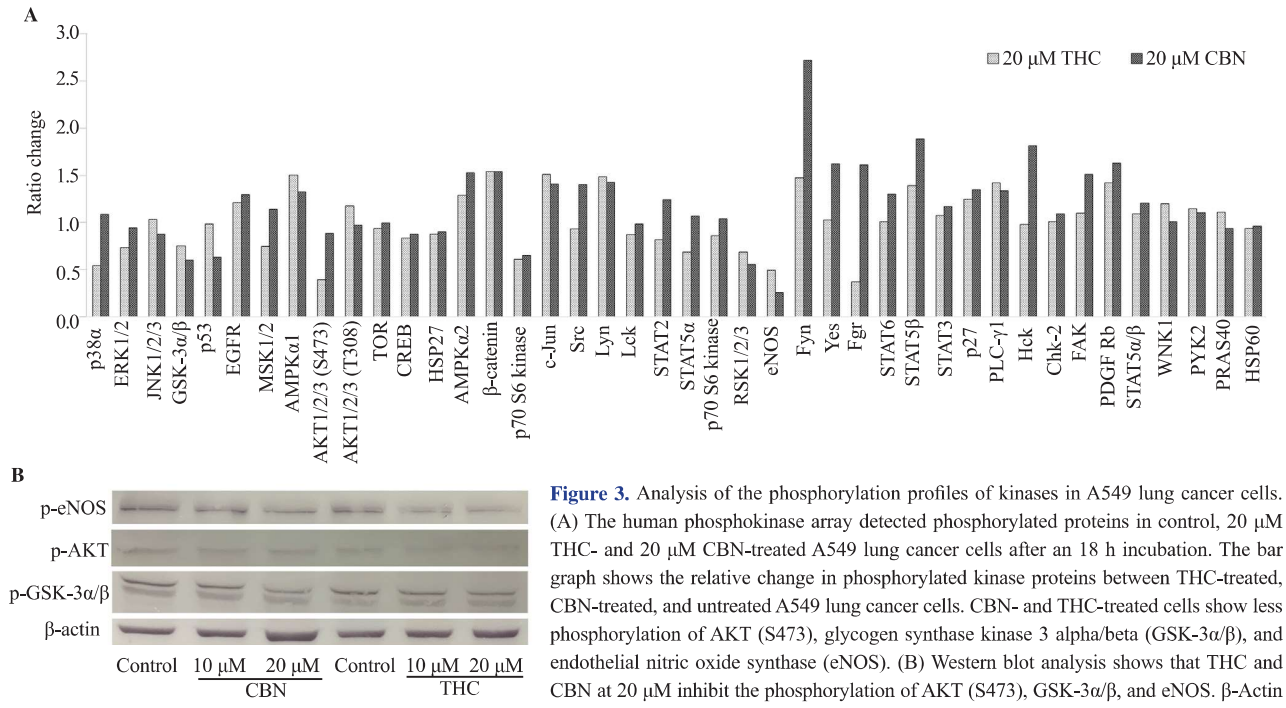

Figure 3. Analysis of the phosphorylation profiles of kinases in A549 lung cancer cells. (A) The human phosphokinase array detected phosphorylated proteins in control, 20 μM THC- and 20 μM CBN-treated A549 lung cancer cells after an 18 h incubation. The bar graph shows the relative change in phosphorylated kinase proteins between THC-treated, CBN-treated, and untreated A549 lung cancer cells. CBN- and THC-treated cells show less phosphorylation of AKT (S473), glycogen synthase kinase 3 alpha/beta (GSK-3α/β), and endothelial nitric oxide synthase (eNOS). (B) Western blot analysis shows that THC and CBN at 20 μM inhibit the phosphorylation of AKT (S473), GSK-3α/β, and eNOS. β-Actin was used as a loading control.

L-NAME also significantly diminished the viability of A549 cells at concentrations of 1, 5, and 10 μM at 24 h (P=0.005 for 1 μM, P=0.007 for 5 μM, and P<0.001 for 10 μM) and 48 h compared to the control cells (P=0.010 for 1 μM, P=0.001 for 5 μM and P<0.001 for 10 μM; Figure 4).

3.5. Effects of THC and CBN on tumor growth in xenograft mice

We subsequently evaluated the effects of CBN and THC *in vivo* after the *in vitro* study showed antiproliferative and apoptotic activity. The daily treatment was applied to the circumference of

the tumor for 20 d (Figure 5A). During treatment, all mice showed normal behavior, and no significant changes were observed in the average body weights of each group (Figure 5B).

On day 20 of the tumor growth curve (Figures 5C and D), the percent tumor changes in mice treated with 15 mg/kg THC (250.63%) or 40 mg/kg CBN (266.00%) were significantly lower than those of the control mice (716.48%; P=0.036 for 15 mg/kg THC and P=0.042 for 40 mg/kg CBN). However, the percentage of tumor changes in xenograft mice treated with 20 mg/kg CBN (344.72%) was lower than the control mice but did not reach statistical significance on day 20.

All mice in the control group had tumor volumes greater than 300 mm^3 on day 20. The mice treated with 15 mg/kg THC and 40 mg/kg CBN showed significantly slower tumor progression (assessed by the number of mice with a tumor volume less than 300 mm^3) than the control group (P=0.012 for 15 mg/kg THC and P=0.042 for 40 mg/kg CBN; Figure 5E). However, no differences were observed in the rate of tumor progression between mice treated with 20 mg/kg CBN and the control mice (P=0.252).

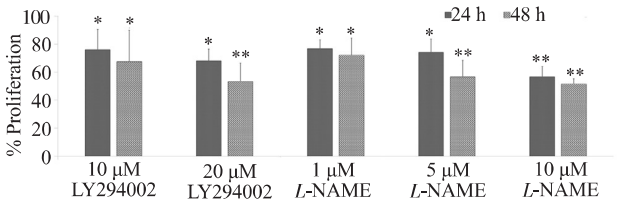

Figure 4. LY294002 and *L*-NAME significantly suppress A549 cell proliferation at 24 and 48 h (ANOVA, $^{*}P$<0.05, $^{**}P$<0.001, compared to the control).

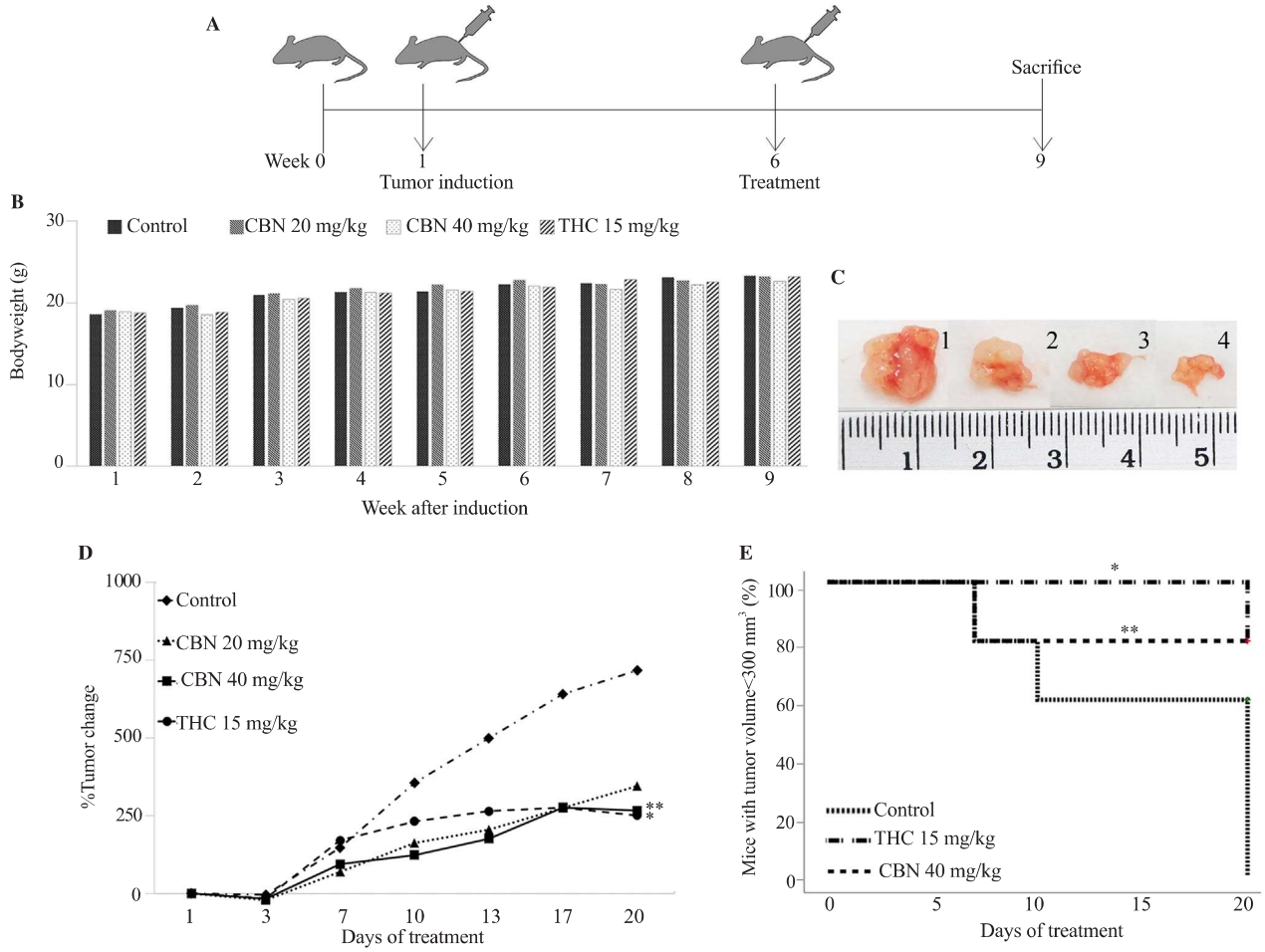

Figure 5. Effects of THC and CBN on tumor growth in A549 xenograft mice. (A) Experimental timeline schematic for the animal experiment. (B) The average body weights of nude mice after tumor induction. (C) Tumors of xenograft mice after treatment with (1) control, (2) 20 mg/kg CBN, (3) 40 mg/kg CBN, and (4) 15 mg/kg THC for 20 d. (D) Tumor growth curves for control, 20 mg/kg CBN-, 40 mg/kg CBN- and 15 mg/kg THC-treated mice. The tumors from A549 xenograft mice treated with 15 mg/kg THC and 40 mg/kg CBN were significantly decreased compared with those of control mice on day 20 (ANOVA, $^{*}P$=0.036 for 15 mg/kg THC and $^{**}P$=0.042 for 40 mg/kg CBN). (E) Tumor progression curve indicating the percentage of mice with tumor volumes less than 300 mm^3. THC at 15 mg/kg and CBN at 40 mg/kg significantly inhibit tumor growth in A549 xenograft mice compared to the control mice (log-rank test, $^{*}P$=0.012 for 15 mg/kg THC and $^{**}P$=0.042 for 40 mg/kg CBN).

3.6. Pathological study of tumor specimens

Hematoxylin and eosin staining of a tumor specimen from a xenograft mouse revealed a multilobulated mass composed of epithelial cell tumors arranged in an acinar pattern. Tumor cells had cuboidal shapes, round nuclei, and prominent nucleoli. Some tumor cells had vacuolate cytoplasm. The tumor cells showed a moderate degree of pleomorphism (Figure 6A).

Immunohistochemical staining of cleaved caspase-3 and cleaved PARP was used to detect apoptosis in the tumor specimens. The tumor specimens from 40 mg/kg CBN-treated mice and 15 mg/kg THC-treated mice showed high levels of cleaved caspase-3 and cleaved PARP, whereas the tumor specimens from control mice showed low levels of cleaved caspase-3 and cleaved PARP.

THC and CBN were found to reduce AKT phosphorylation in cell culture studies. Thus, immunohistochemistry was used to detect AKT phosphorylation in the tumor specimens. The results showed that tumor samples from the control mice had high levels of AKT phosphorylation, while tumor specimens from mice treated with 40 mg/kg CBN or 15 mg/kg THC showed low levels of AKT phosphorylation (Figure 6B).

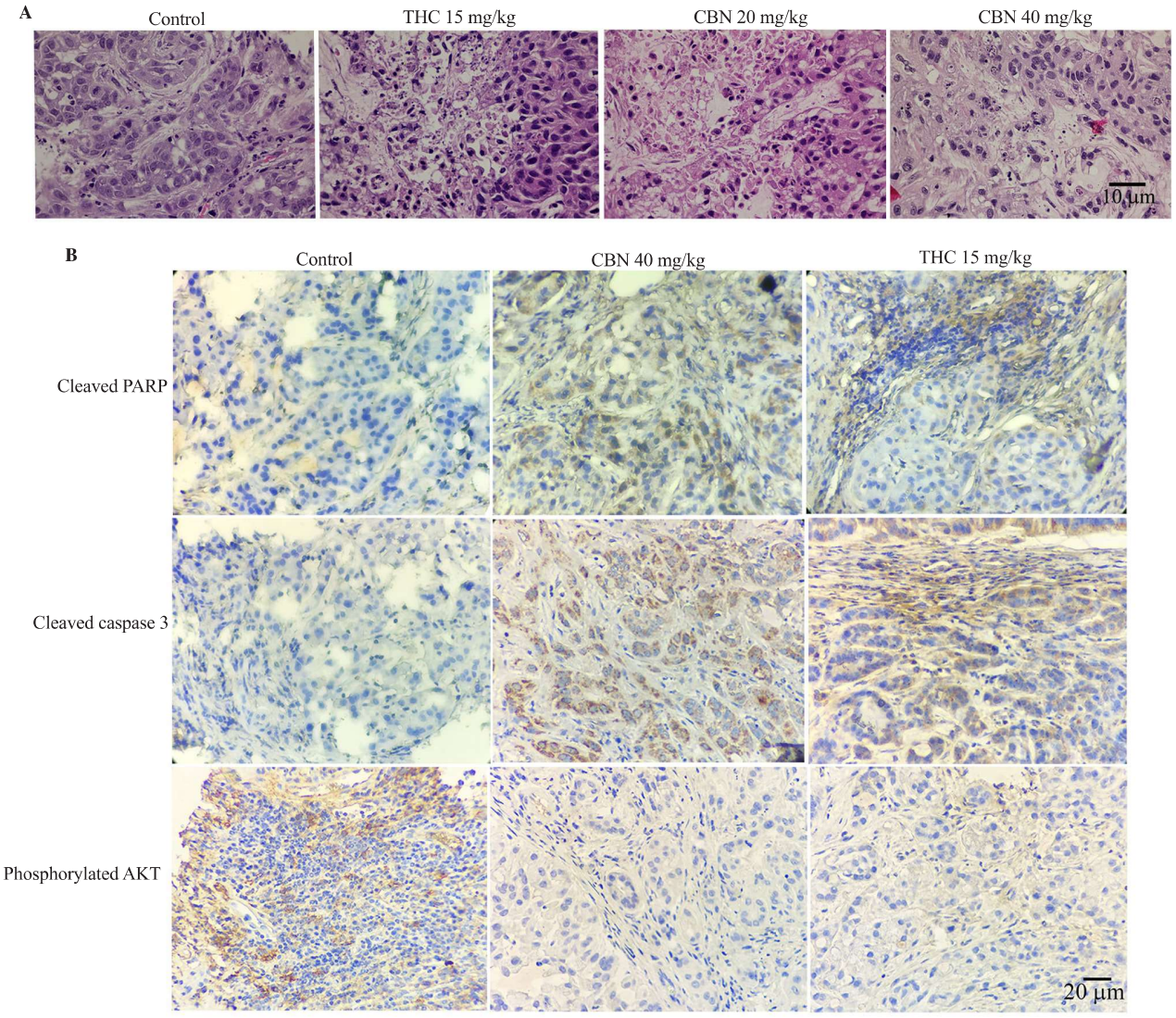

Figure 6. Pathological study of tumor specimens from A549 xenograft mice. (A) Hematoxylin and eosin staining of the xenograft tumor. The specimens were composed of epithelial cell tumors arranged in an acinar pattern. Magnification, × 400; scale bars, 10 μm. (B) Immunohistochemical staining of xenograft mouse specimens treated as indicated. Cleaved PARP and cleaved caspase-3 signaling were strongly detected in the specimens from xenograft mice treated with 15 mg/kg THC or 40 mg/kg CBN. Phosphorylated AKT was barely expressed in the specimens from xenograft mice treated with 15 mg/kg THC or 40 mg/kg CBN compared to the specimens from the control mice. Magnification ×400; scale bars, 20 μm.

4. Discussion

Cannabinoids from *Cannabis sativa* can inhibit proliferation, metastasis, and angiogenesis in various cancer models[4–6]. The effects of THC, the major psychoactive component of *Cannabis sativa*, in the central nervous system are mediated by the CB1 receptor. Despite the psychoactive effects of THC, many studies have demonstrated the anticancer potential of THC in various cancer cells[11]. CBN is a mildly psychoactive cannabinoid that is derived from THC and is mostly found in aged and stored *Cannabis sativa*. A previous study demonstrated that CBN has a higher affinity for the CB2 receptor[9]. Previous research has also shown that CB1 and CB2 receptors are expressed in NSCLC cells[12]. This study investigated the effects of CBN in human lung cancer cells. Anticancer effects of CBN were observed in both *in vitro* and *in vivo* studies.

According to our findings from the proliferation assay, THC inhibited lung cancer cell proliferation, which is consistent with previous research[12]. CBN also inhibited A549 cell proliferation in a concentration-dependent manner. In addition, flow cytometry using annexin V showed that THC and CBN induced apoptosis in A549 cells, and THC induced more apoptosis than CBN at 10 μM and 20 μM. Western blot analysis also demonstrated an increase in cleaved PARP in THC- and CBN-treated human lung cancer cells. Taken together, these results indicate that both THC and CBN induce apoptosis in human lung cancer cells.

It was also found that treatment with THC or CBN decreased the phosphorylation of AKT both *in vitro* and *in vivo*. Treatment with these compounds also decreased the phosphorylation of GSK-3α/β in A549 cells. GSK-3β is a serine/threonine-protein kinase that is involved in glucose metabolism. Many studies have shown that GSK-3β has different roles in the cellular processes of human cancer, including cell proliferation and death, and the regulation of gene transcription and protein expression. In its activated state, GSK-3β inhibits β-catenin, which inhibits cell proliferation[13].

In contrast to most other kinases, phosphorylation of GSK-3β is the inactive state and is mainly regulated by AKT, thereby promoting cell proliferation[14–16]. Previous research has shown that GSK3 inhibits mTOR activity, which reduces cell proliferation[17]. AKT phosphorylates GSK3, which is then inactivated by targeted proteasome degradation. As a result of GSK3 inactivation, mTOR is activated, which leads to increased cell proliferation[18]. We hypothesize that the apoptosis of A549 cells treated with THC or CBN is caused by decreased phosphorylation of AKT, which results in decreased phosphorylation of GSK-3α/β. Indeed, this has been confirmed by a previous study where it was found that THC decreased the level of phosphorylated GSK-3β[19].

Nitric oxide (NO) plays a role in cancer initiation and progression. NOS creates NO from *L*-arginine, NADPH, and oxygen[20]. eNOS, a key isoform of NOS, is involved in the development of cancer[21]. PI3K/AKT acts as an upstream regulatory signal for eNOS[22]. Previous research has found that PI3K-AKT signaling leads to eNOS phosphorylation at S1177, which stimulates Ras family members and increases cancer cell growth[21]. In the current study, THC and CBN treatment of A549 cells resulted in lower phosphorylation of eNOS and AKT compared to controls. Furthermore, we found that *L*-NAME, an eNOS-specific inhibitor, could inhibit the proliferation of A549 cells.

THC and CBN inhibited lung cancer cell growth by inhibiting AKT and its signaling pathways, which include GSK-3α/β and eNOS. THC and CBN also significantly inhibited tumor growth in an animal model. In addition, immunohistochemistry detected cleaved caspase-3 and cleaved PARP in tumor specimens. These data provide evidence that THC and CBN induce lung tumor apoptosis in xenograft mice. The phosphorylation of AKT was significantly decreased in tumor specimens from xenograft mice treated with THC or CBN. This finding is supported by a previous study that showed that THC reduces the growth of breast tumors in xenograft mice[23].

The study limitation is that using only one cell line may be inaccurate. Further research employing a variety of cell lines or primary cancer cells is required.

In summary, these findings show that THC and CBN can inhibit lung cancer cell growth by inhibiting AKT, GSK-3α/β, and eNOS. More research should be conducted on the efficacy of THC and CBN when combined with EGFR-TKIs in NSCLC patients with PI3K-related mutations.

Conflict of interest statement

The authors declare no conflict of interest.

Acknowledgments

The authors would like to thank Miss Sukanya Settharaksa, Mr. Tak Karuncharoenpanich, and Miss Sulakkhana Suporn at the College of Pharmacy, Rangsit University, for the cell culture and animal work, and Miss Luxsana Panrit and Miss Phunuch Muhamad at the Drug Discovery and Development Center, Thammasat University, for their technical assistance with flow cytometry and UVP ChemStudio.

Funding

This study was funded by a grant from the Research Institute, Rangsit University (grant number 103/2561, 2018) and by the College of Pharmacy, Rangsit University.

Authors' contributions

SL and KL designed and organized the study, analyzed the results, and prepared the main manuscript text. SL worked with the animals. SL and TW set up the cell culture and molecular laboratory. WS prepared the sample injections for the mouse experiment. NK analysed THC and CBN. FM, AM, PP, and LS extracted and separated the THC and CBN. TS reviewed and criticized manuscript. KL evaluated the statistical analysis.

References

[1] Bray F, Ferlay J, Soerjomataram I, Siegel RL, Torre LA, Jemal A. Global cancer statistics 2018: GLOBOCAN estimates of incidence and mortality worldwide for 36 cancers in 185 countries. *CA Cancer J Clin* 2018; **68**: 394-424.

[2] Molina JR, Yang P, Cassivi SD, Schild SE, Adjei AA. Non-small cell lung cancer: Epidemiology, risk factors, treatment, and survivorship. *Mayo Clin Proc* 2008; **83**(5): 584-594.

[3] Fang W, Huang Y, Gu W, Gan J, Wang W, Zhang S, et al. PI3K-AKT-mTOR pathway alterations in advanced NSCLC patients after progression on EGFR-TKI and clinical response to EGFR-TKI plus everolimus combination therapy. *Transl Lung Cancer Res* 2020; **9**(4): 1258-1267.

[4] Hinz B, Ramer R. Anti-tumour actions of cannabinoids. *British J Pharmacol* 2019; **176**: 1384-1394.

[5] Afrin F, Chi M, Eamens AL, Duchatel RJ, Douglas AM, Schneider J, et al. Can Hemp help? Low-THC cannabis and non-THC cannabinoids for the treatment of cancer. *Cancers* 2020; **12**: 1033.

[6] Śledziński P, Zeyland J, Słomski R, Nowak A. The current state and future perspectives of cannabinoids in cancer biology. *Cancer Med* 2018; **7**(3): 765-775.

[7] Leelawat S, Leelawat K, Narong S, Matangkasombut O. The dual effects of delta (9)-tetrahydrocannabinol on cholangiocarcinoma cells: Anti-invasion activity at low concentration and apoptosis induction at high concentration. *Cancer Invest* 2010; **28**(4): 357-363.

[8] Murray RM, Englund A, Abi-Dargham A, Lewis DA, Forti MD, Davies C, et al. Cannabis-associated psychosis: Neural substrate and clinical impact. *Neuropharmacol* 2017; **124**: 89-104.

[9] Morales P, Hurst DP, Reggio PH. Molecular targets of the phytocannabinoids-A complex picture. *Prog Chem Org Nat Prod* 2017; **103**: 103-131.

[10]Choi YH, Hazekamp A, Peltenburg-Looman AMG, Frédérich M, Erkelens C, Lefeber AWM, et al. NMR assignments of the major cannabinoids and cannabiflavonoids isolated from flowers of *Cannabis sativa*. *Phytochem Anal* 2004; **15**(6): 345-354.

[11]Tomko AM, Whynot EG, Ellis LD, Dupre DJ. Anti-cancer potential of cannabinoids, terpenes, and flavonoids present in cannabis. *Cancers* 2020; **12**(7): 1985.

[12]Milian L, Mata M, Alcacer J, Oliver M, Sancho-Tello M, Martín de Llano JJ, et al. Cannabinoid receptor expression in nonsmall cell lung cancer. Effectiveness of tetrahydrocannabinol and cannabidiol inhibiting cell proliferation and epithelial mesenchymal transition *in vitro*. *PLoS One* 2020; **15**(2): e0228909.

[13]Duda P, Akula SM, Abrams SL, Steelman LS, Martelli AM, Cocco L. Targeting GSK3 and associated signaling pathways involved in cancer. *Cells* 2020; **9**: 1110.

[14]Liu M, Huang X, Tian Y, Yan X, Wang F, Chen J, et al. Phosphorylated GSK-3β protects stress-induced apoptosis of myoblasts *via* the PI3K/Akt signaling pathway. *Mol Med Rep* 2020; **22**: 317-327.

[15]Stamos JL, Weis WI. The β-catenin destruction complex. *Cold Spring Harb Perspect Biol* 2013; **5**(1): a007898.

[16]Karim R, Tse G, Putti T, Scolyer R, Lee S. The significance of the Wnt pathway in the pathology of human cancers. *Pathology* 2004; **36**(2): 120-128.

[17]Yohn NL, Bingaman CN, DuMont AL, Yoo LI. Phosphatidylinositol 3'-kinase, mTOR, and glycogen synthase kinase-3beta mediated regulation of p21 in human urothelial carcinoma cells. *BMC Urol* 2011; **11**: 19.

[18]Nagini S, Sophia J, Mishra R. Glycogen synthase kinases: Moonlighting proteins with theranostic potential in cancer. *Semin Cancer Biol* 2019; **56**: 25-36.

[19]Cao C, Li Y, Liu H, Bai G, Mayl J, Lin X, et al. The potential therapeutic effects of THC on Alzheimer's disease. *J Alzheimers Dis* 2014; **42**(3): 973-984.

[20]Robbins RA, Grisham MB. Nitric oxide. *Int J Biochem Cell Biol* 1997; **29**(6): 857-860.

[21]Lim KH, Ancrile BB, Kashatus DF, Counter CM. Tumour maintenance is mediated by eNOS. *Nature* 2008; **452**(7187): 646-649.

[22]Kanwar JR, Kanwar RK, Burrow H, Baratchi S. Recent advances on the roles of NO in cancer and chronic inflammatory disorders. *Review Curr Med Chem* 2009; **16**(19): 2373-2394.

[23]Caffarel MM, Andradas C, Mira E, Pérez-Gómez E, Cerutti C, Moreno-Bueno G, et al. Cannabinoids reduce ErbB2-driven breast cancer progression through Akt inhibition. *Mol Cancer* 2010; **9**: 196.